

## Data Fusion Issues in Analysing Coastal Morphodynamic Systems

D. G. Bailey and R. D. Shand  
Physics Department and Geography Department  
Massey University, Palmerston North, New Zealand  
E-mail: D.G.Bailey@massey.ac.nz, R.D.Shand@clear.net.nz

### Abstract

*This paper describes a range of coastal data acquisition techniques and discusses some of the associated data fusion issues. To better understand the form and process dynamics at the interface between land and ocean, there is a need for comprehensive data. Traditional water contact methods of acquiring morphological data such as echo-sounding are discussed, and some of the more recent remote techniques incorporating photographic and video imaging are described. The inherent differences in the calibration requirements for data acquired by these methods are considered based on field results from Wanganui, New Zealand. Reconciling such differences may be important, and this can enable data sets to be extended both spatially and temporally. Comparison of contemporaneous data is carried out to identify systematic errors and develop corresponding compensation corrections.*

**Keywords:** data fusion, sandbars, time-exposure, echo-sounding, time-stacks

### 1. Introduction

There is a growing need to understand coastal systems and how they change with time. Of particular interest is the 'active zone', that area of the coast subjected to wave influenced sediment transport [1]. This zone is highly dynamic and unstable with erosion exceeding deposition globally [2]. A variety of topographical data acquisition techniques have been developed for the coastal active zone [3,4]. The method selected is determined by the physical environment, the resolution and accuracy required, and the available equipment, skill and manpower.

There is often a need to combine data sets obtained under different environmental conditions or by different acquisition methods. Such data fusion may be required to increase the record length, to extend the spatial coverage, to enable intersite comparison where different data acquisition methods were used, or to increase the quality of the data by identifying and correcting systematic errors. Each technique has its own interpretation and error limitations which must be identified and accounted for when data sets are combined for use in morphodynamic (interactions between form and process) analysis.

This paper describes a range of data acquisition

techniques and some of the data fusion issues that we have encountered at Wanganui, on the south west coast of the North Island, New Zealand. The site includes the Wanganui river mouth and 5 km of adjacent coast to the west as shown in figure 1. The active zone is approximately 400 m wide.



**Figure 1:** An aerial photograph of the field site with the Wanganui river breakwaters in the foreground, and the cliffs used as the camera platform in the upper right.

## 2. Data Acquisition Methods

### 2.1 Echo soundings

The river mouth is echo-sounded monthly by the Port Company for navigational purposes (figure 2(a)). Sounding requires low sea and wind conditions. A bathymetric chart covering 200 m by 600 m is produced from the survey output at 20 m resolution (figure 2(b)). Errors are  $\pm 0.3$  m elevation and  $\pm 5$  to 10 m position. An image is produced from each chart by digitising traced contour maps with contours drawn at 0.5 m intervals (figure 2(c)).

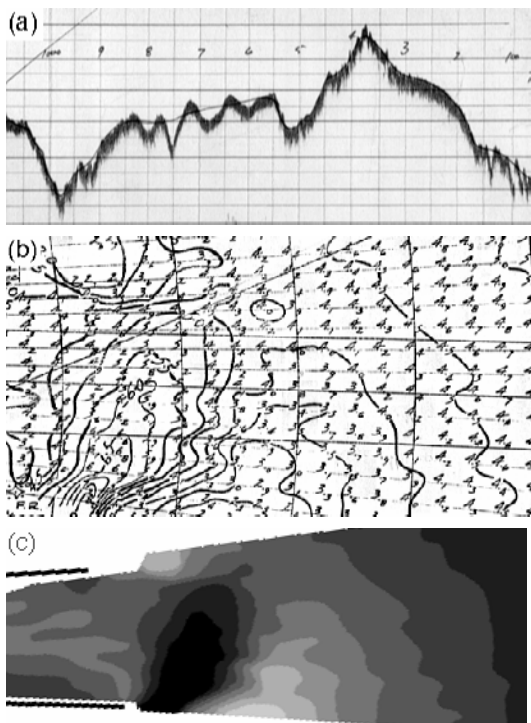


**Figure 2:** Echo sounding data. (a) A trace of the echo along the central profile. (b) Several profiles combined to make a bathymetric chart. (c) The depth contours are digitised and converted to give a depth map image.

On the coast, cross-shore transits at 200, 1600, and 5000 m to the west of the river mouth were surveyed at three monthly intervals by echo-sounding and levelling using a theodolite. Echo-sounding was carried out seaward of the low tide mark between July 1991 and October 1993. Errors are  $\pm 0.3$  m elevation and  $\pm 5$  to 10 m position. The intertidal beach was levelled between December 1989 and May 1994. Errors are  $\pm 0.025$  m elevation and  $\pm 2.5$  m position. The sonar and levelling data were merged. The location of the bar crests were determined using the common method of fitting a power curve to the profile and determining the

locations of maximum residuals [5] as shown in figure 3. The active zone can be identified from the profile envelope, and standard deviations about the mean profile.

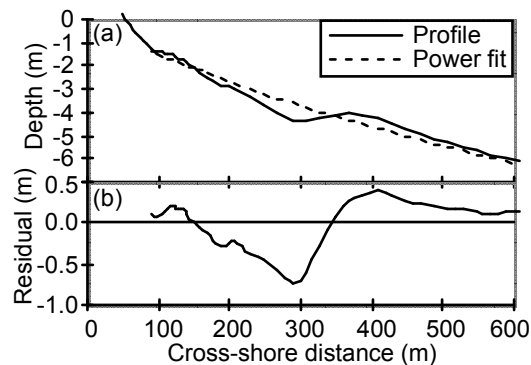


**Figure 3:** (a) A sounding profile with power curve fitted. (b) Residuals with maxima indicating bar crests.

### 2.2 Aerial photography

The river mouth and coast were surveyed by vertical aerial photography on 8 occasions between August 1991 and July 1993. Such aerial photography required clear skies and waves large enough to break on all sandbars (greater than 2 m). The photographs (one of which is shown in figure 4) were digitised, rectified using a series of surveyed ground control points, and mosaiced to produce a composite image of the study site (as in figure 10(a)). Position errors on the sea surface are  $\pm 12$  m. As wave breaking is depth dependent, the location of a bar crest is inferred on the images from the positions of local maximum intensity. Elevation is therefore only known in a relative sense. Environmental variables such as wave height and sea level at the time of sampling influence the inferred crest location.

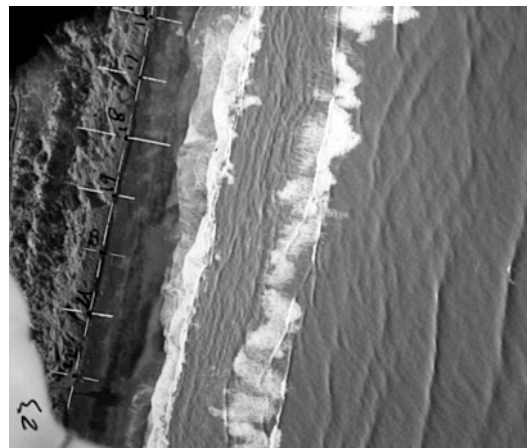


**Figure 4:** One of a sequence of vertical aerial photographs. Crosses locate ground control points at 100 m intervals.

### 2.3 Time-exposure photography

Photographic techniques using long exposure times have been developed to reduce the effects of wave height modulation [6]. At the study sight, multiple wave trains are often present (for example, see figure 1), and ocean wave heights often have a Rayleigh distribution. The breakpoint therefore varies, and this introduces a random error when locating bar crests using intensity maxima from instantaneous photographs (compare figures 5(a) and 5(b)). The study site was surveyed by oblique terrestrial time-exposure (4 minutes) photography at monthly intervals between June 1992 and June 1996. The photographs were digitised, rectified, and mosaiced to produce composite images as shown in figure 5(c) [7,8]. The environmental errors that apply to aerial images also apply to the time exposure images. For the study site, the offshore error is approximately  $\pm 10$  m. The longshore error deteriorates rapidly with distance from the camera. There are three main sources of longshore error which all vary approximately linearly with distance: pixel resolution of captured images ( $\pm 40$  m at 3 km); photogrammetric errors ( $\pm 60$  m at 3 km); and an offset caused by the height of the waves ( $\pm 75$  m at 3 km). As these error sources are independent, the corresponding variances may be added to give a longshore error

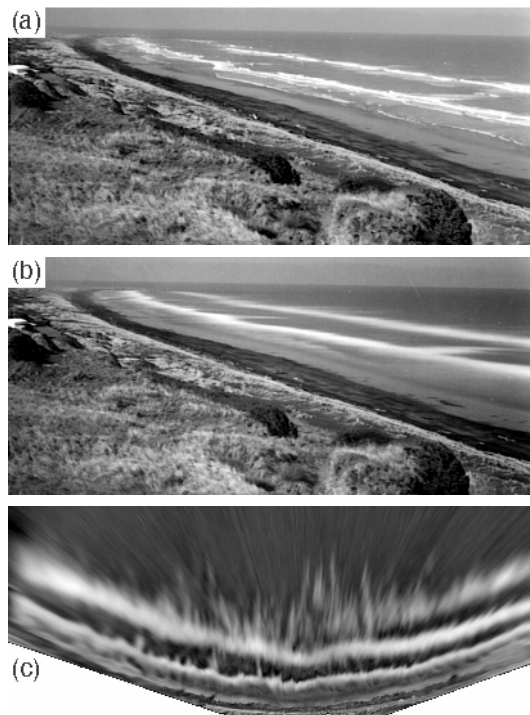


**Figure 5:** Oblique terrestrial photographs. (a) An instantaneous photograph showing individual waves. (b) A 4 minute time exposure. (c) A mosaic of 8 photographs spanning 5 km (offshore scale x2).

of  $\pm 2$  m directly out from the camera up to  $\pm 100$  m at a distance of 3 km.

### 2.4 Video techniques

Oblique terrestrial videos were captured of waves breaking on the bars opposite the camera (figure 6(a)) to obtain intensity inferred morphological data and also hydrodynamic data over a small area. The intensity data on the 3200 m transit was captured from the video images at 0.25 second intervals to form a time-stack or image of what happened on that transit as a function of time [9]. Such video time-stacks (for example figure 6(b)) clearly show the wave height modulation effects. A time-stack taken over the tidal cycle shows the movement of the inferred crest location as the sea level changes. Low frequency wave motions can be detected using intensity patterns on the bars and beach face. Alternatively, time averaging video frames gives a time exposure image equivalent to the photographic long exposure.

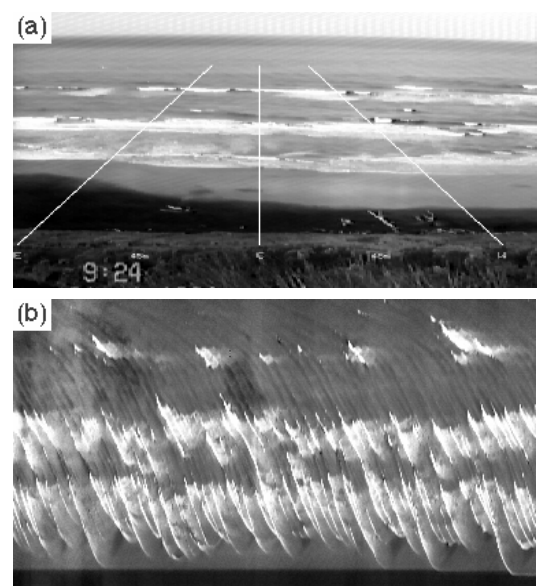


**Figure 6:** (a) A single video frame showing three shore normal transits. (b) A 6 minute time-stack taken from the central transit.

### Data Fusion Issues:

Terrestrial time-exposure photography or video are the preferred data acquisition methods because they allow large areas to be surveyed, are easily automated, relatively cheap to operate and function under a wide range of environmental conditions. The disadvantage is that there is no quantitative information on depth, and the detected bar locations need to be adjusted for environmental conditions.

Environmental factors influencing wave breaking include: incident wave height, low frequency (>20 s) wave heights, tide level, wind or pressure storm surges, and morphological configuration. Figure 7 shows rectified time exposure images sampled 24 hours apart. Wind, barometric pressure, tide level, and wave period remained approximately constant. Changes in incident wave height (2.2 to 1.2 m), wave setup, low frequency surges, and differences in the morphological configuration are responsible for the movement of intensity maxima as indicated in figure 7(c). While significant spatial variation occurs (compare (i) and (ii)) this can be reduced by longshore averaging (as in (iii)).

The tide shift translates the intensity pattern cross-shore in response to changing depth (figure 8). Some of the fluctuation in the detected intensity maxima locations (figure 8(b)) can be attributed to

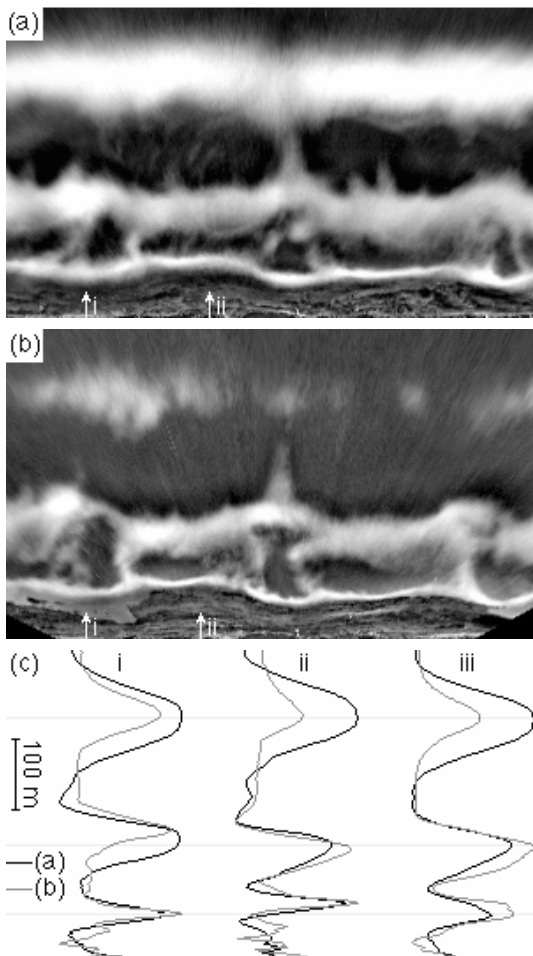


**Figure 7:** Effect of wave height change on intensity distribution (offshore scale x2). (a) 2.2 m. (b) 1.2 m. (c) i) & ii) Intensity profiles of indicated positions (averaged over 150 m), iii) Intensity profile averaged over 1500 m.

low frequency sea level oscillations. Spectral and time series analyses at Wanganui have consistently shown that such oscillations range in period from 30 seconds to over 60 minutes. However, most of the energy occurs at periods less than 15 minutes, so time averaging over this interval significantly reduces this source of random error.

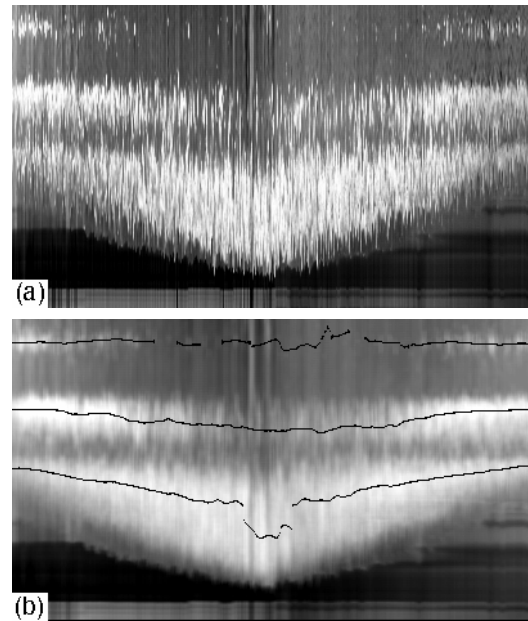


**Figure 8:** Effect of sea level (tide) on intensity maxima positions. (a) A compressed time stack taken over 6 hours including high tide. (b) The same time stack with a 4 minute running average. Superimposed are the detected intensity maxima.

The incident wave height also offsets the intensity maximum away from the camera as illustrated in figure 9.

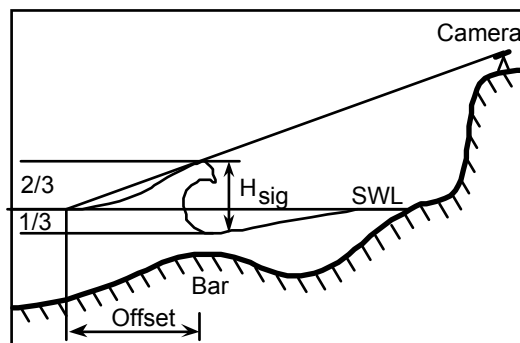


**Figure 9:** The effects of wave height on apparent breaker position.

The different types of data obtained from different sources allows systematic errors to be identified, and an empirical correction applied. For example, the photogrammetric errors associated with the vertical aerial images are uniformly distributed, while those associated with the oblique time-

exposure images vary significantly with distance from the camera. Any differences between images captured using the two methods at the same time can be attributed to the rectification model used with the oblique time-exposure images. Figures 10(a) and (b) show corresponding aerial and terrestrial long exposure images. An error surface figure 10(c) was fitted to the location differences between corresponding intensity maxima in several such pairs. This allows such systematic errors to be removed from time exposure data.

Comparing oblique time-exposure intensity profiles with echo-soundings enables correspondence between the inferred bar-crest and the actual bar-crest to be determined. By comparing time-averaged bar-crest locations with time-averaged ground profiles, contamination by environmental variables is eliminated. Figure 11 shows the differences between these crests as a function of depth for the measured transits. The relationship shows that landward intensity maxima

are displaced offshore, while seaward intensity maxima are displaced onshore. This result is consistent with the depth control over wave breaking.

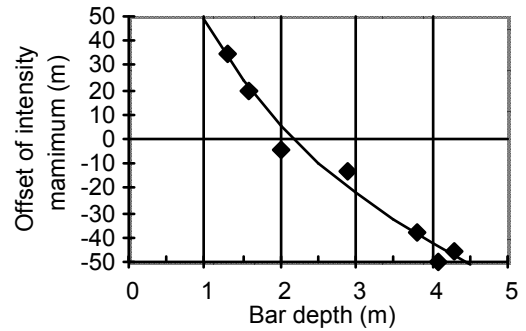


**Figure 11:** Image to ground survey crest location offsets as a function of depth, taken from transits at 200, 1600 and 5000 m.

What happens at the river mouth is of primary interest for navigation. The oblique time exposure method does not adequately image the river mouth as it is too far away from the camera site, it is partially obscured by the mole, and the water is too deep for the waves to break reliably. Extending the data set spatially to include the river mouth involves combining the available bathymetric data with the image data. In spite of the fact that these data sets contain different types of information, the relationship between the sandbars adjacent to the river mouth and the deeper bars within the river

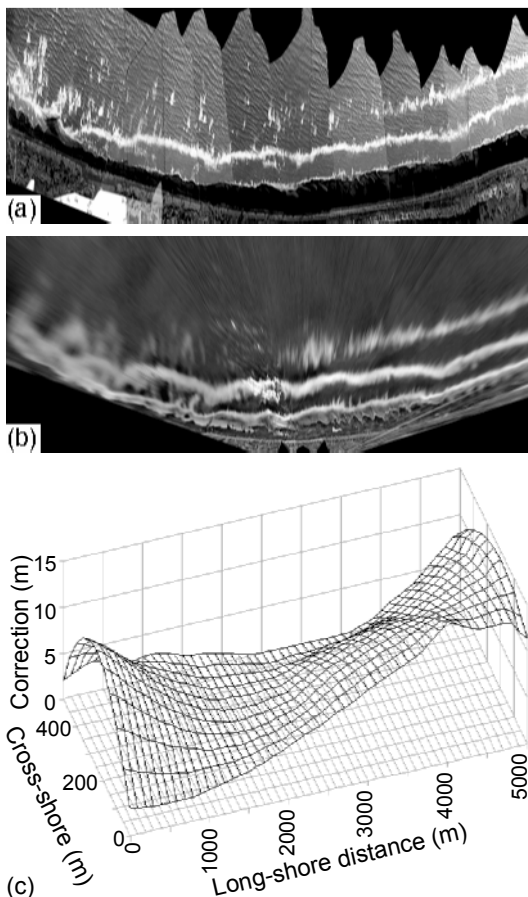


**Figure 10:** Sea surface intensity accuracy. (a) An example of a vertical aerial mosaic (offshore scale x2). (b) The corresponding terrestrial long exposure mosaic (offshore scale x2). (c) The error surface found empirically by comparing several such sets of data.

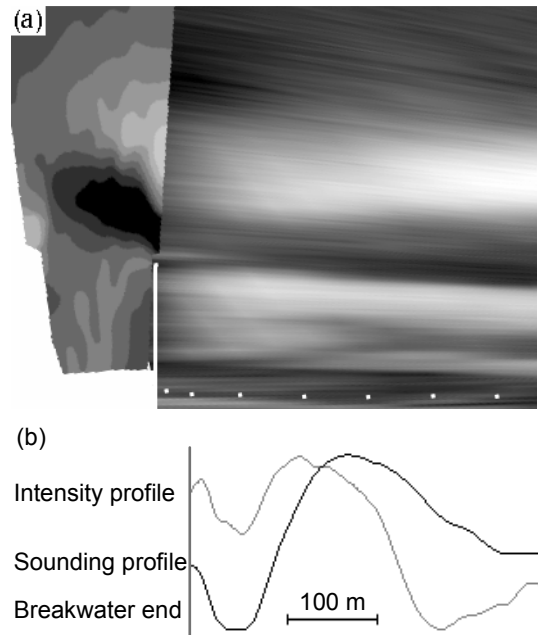


**Figure 12:** River mouth data fusion. (a) The sounding depth image overlaid on the rectified long exposure image. (b) Comparison of adjacent sounding and intensity profiles beyond then end of the breakwater.

mouth is readily apparent in figure 12(a). While the bathymetric data locates the bar crest by minimum depth rather than by the power residual method, and the systematic correction of figure 10(c) has not been applied, the landward offset of the coastal image intensity maximum figure 12(b) is in agreement with that predicted from figure 11(b).

When investigating coastal morphodynamics, it is important to determine the movement of the bar locations with time. One convenient method of analysing this data is to view the data at a particular transit as a function of time, using a timestack. However, the contrast of the input images varies (figure 13(a)) depending on reflection (the sun angle, and whether or not it is cloudy), wave height (smaller waves do not break as strongly, and produce less foam), and different lens speeds (the different lenses for near and far photographs produce images with different contrasts). To overcome this, the individual images are normalised (figure 13(b)) prior to constructing the timestack by shaping their histograms to the average histogram over the whole sequence. A typical normalised and filtered time-stack is shown in figure 13(c), illustrating the net offshore migration of the sandbars with time.

#### 4. Summary

The availability of data and images from several different sources can be used to improve the overall quality and quantity of the data. The different sources are subject to different systematic errors and environmental influences. Comparing data from different sources can enable systematic and environmental errors to be identified and removed. The spatial or temporal coverage may be extended by utilising all the data available, although special consideration needs to be taken when combining data from disparate sources to

ensure that the data is compatible.

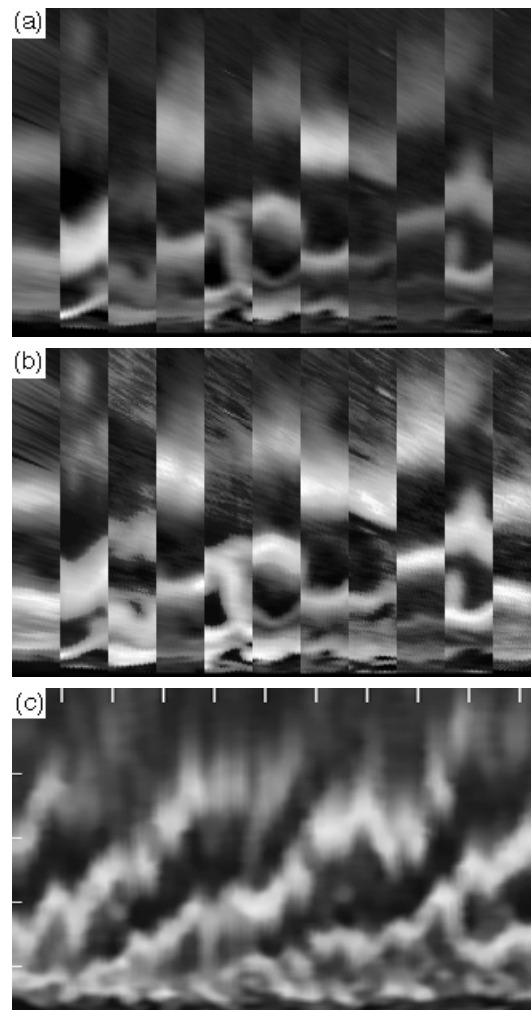


**Figure 13:** Image normalisation for time stack construction. (a) Slices from a series of images showing variations in brightness and contrast. (b) The same slices after intensity normalisation. (c) The resultant time stack from monthly data over 4 years.

#### References

- [1] R.J. Hallermeier, "Sand Transport Limits in Coastal Structure Design", Proceedings Coastal Structures '83, 703-716, 1983.
- [2] E.C.F. Bird, *Coastline Changes: A Global View*, John Wiley & Sons, London, 1985.
- [3] R.A. Holman & A.H. Sallenger, "High energy nearshore processes", EOS Trans. AGU 67, 1369-1371, 1986.
- [4] K. Horikawa, *Nearshore Dynamics and Coastal Processes*, University of Tokyo Press, 1988.
- [5] A.J. Bowen & R.A. Holman, "Bars, bumps, and holes: models for the generation of complex beach topography", *Journal of Geophysical Research*, 84, 457-468, 1982.
- [6] T.C. Lippman & R.A. Holman, "Quantification of Sand Bar Morphology: A Video Technique Based on Wave Dissipation", *Journal of Geophysical Research*, 94, 995-1011, 1989.
- [7] D.G. Bailey & R.D. Shand, "Determining Large Scale Sandbar Evolution", Proceedings 1st NZ Conference on Image and Vision Computing, 109-116, 1993.
- [8] D.G. Bailey & R.D. Shand, "Determining Large Scale Sandbar Behaviour", Proceedings IEEE International Conference on Image Processing, 2, 637-640, 1996.
- [9] D.G. Bailey & R.D. Shand, "Determining Wave Run-up using Automated Video Analysis", Proceedings 2nd NZ Conference on Image and Vision Computing, 2.11.1-2.11.10, 1994.